applied sciences

MDPI

Article

Experimental Validation of a Longitudinal Vehicle Model for an Agricultural Vehicle Using Coast-Down Testing and Diagnostic Data

Ugnė Koletė Medževeprytė [1,*], Rolandas Makaras [1,*], Vaidas Lukoševičius [1] and Algirdas Laskys [2]

[1] Faculty of Mechanical Engineering and Design, Kaunas University of Technology, Studentų Str. 56, 51424 Kaunas, Lithuania; vaidas.lukosevicius@ktu.lt
[2] Independent Researcher, Kuršių Str. 12, 48147 Kaunas, Lithuania
* Correspondence: ugne.medzevepryte@ktu.lt (U.K.M.); rolandas.makaras@ktu.lt (R.M.)

Featured Application

Work described in this article is a part of the creation of the Hybrid Operational Cycle—a unified methodology to evaluate an off-road heavy-duty vehicle what work in various terrains and perform a broad spectre of specified tasks.

Abstract

Accurate modelling of agricultural vehicles is essential for optimizing drivetrain performance and energy efficiency, particularly as hybrid systems become more prevalent in sustainable farming. This study presents an experimental validation of a vehicle physical model using the Claas Xerion 3800 tractor. Coast-down tests were conducted to determine the rolling resistance coefficient, while GPS and diagnostic data were used to capture real-world vehicle dynamics and fuel consumption. The rolling resistance coefficient was calculated using two-stage aggregation method of multiple run data, yielding a statistically robust result. Simulation outputs showed close agreement with measured longitudinal responses, including vehicle acceleration, traction force, and fuel usage, with a 2.1% deviation in total fuel consumption. These findings demonstrate that the proposed modelling approach reliably replicates the vehicle's macroscopic longitudinal dynamics and support its application in drivetrain optimization, hybrid system integration, and energy-efficient vehicle design studies. The validated framework contributes to the development of context-aware simulations capable of reflecting real-world off-road conditions and operational variability.

Keywords: longitudinal dynamics modelling; rolling resistance coefficient; agricultural vehicle simulation; physical model validation; off-road vehicle dynamics

Academic Editors: Ján Dižo, Alyona Lovska and Miroslav Blatnický

Received: 7 January 2026
Revised: 6 February 2026
Accepted: 8 February 2026
Published: 12 February 2026

1. Introduction

In applied engineering—particularly within the agricultural sector—the development of accurate vehicle models is essential to ensure machinery operates efficiently under a variety of conditions. As the demand for sustainable farming practices grows, the hybridization of agricultural machinery has gained significant attention. These hybrid systems offer enhanced fuel efficiency, reduced emissions, and improved adaptability—crucial for modern agriculture, where machinery must perform reliably across diverse and unpredictable environments [1,2].

Recent literature emphasizes the importance of developing reliable and precise vehicle models to simulate real-world performance, especially in off-road contexts [2,3]. Integrating hybrid powertrains into CVT-equipped vehicles, such as tractors, requires a comprehensive modelling approach that accounts for variables ranging from terrain conditions to fluctuating loads [4,5]. Physical modelling plays a vital role in this process, bridging the gap between theoretical simulations and practical applications [6,7]. Model validation ensures that virtual predictions align with actual operational behaviour, making simulation outcomes trustworthy and applicable [8,9].

Modelling and validating hybrid systems in heavy-duty off-road vehicles—such as tractors and military transporters—presents unique challenges. While many studies have explored hybridization, relatively few have addressed the verification of these models under real-world conditions, particularly in off-road settings where terrain and operational loads are constantly changing [10,11]. This gap highlights a critical issue: the difficulty of validating physical models that accurately represent the complex forces and interactions in off-road environments [12,13]. For example, agricultural tractors often operate on uneven, unstructured terrain while performing tasks of varying intensity and type, making their movement difficult to standardize [3]. Traditional modelling approaches, which rely on controlled environments, struggle to capture this variability [14]. Therefore, achieving robust and context-aware simulations that reflect real-world vehicle behaviour remains a key research priority [15].

Reliable data acquisition is essential for model validation, yet collecting consistent, high-quality data in off-road environments remains a major challenge [10,16]. Agricultural practices and vehicle usage vary widely across regions, increasing the need for context-specific data. In Europe, for instance, hybrid systems in agricultural machinery have been the focus of several studies, driven by goals to reduce emissions and improve energy efficiency [17,18]. Similar trends are evident in North America, where research aims to optimize hybrid powertrains for off-road vehicles [3,9,10]. Despite these efforts, challenges in data collection and environmental variability persist. Farming machinery must operate across diverse terrains—from flat fields to rolling hills—and under fluctuating workloads, which complicates the validation process. Physical models must account for dynamic inputs such as soil resistance, crop density, and task-specific mechanical demands, all of which vary significantly depending on the operation being performed [17].

A key obstacle in achieving accurate simulations lies in the model's ability to respond dynamically to real-time changes in vehicle performance, which are heavily influenced by environmental and operational factors [9,11]. To address this, recent research has focused on improving data acquisition techniques. Remote sensing technologies like LiDAR and GPS-based systems have shown promise in capturing precise data under off-road conditions [16]. Additionally, machine learning algorithms are being used to enhance model adaptability by integrating large, diverse datasets and optimizing simulations in real time [17,19]. Nevertheless, the complexity of off-road environments—where variables such as soil composition, weather, and terrain steepness fluctuate—continues to pose significant challenges for hybrid vehicle model validation [2].

Workload variability is particularly impactful in agricultural contexts. Tasks such as ploughing, seeding, harvesting, and transporting differ not only in mechanical demand but also in duration, speed, and required torque. These variations influence energy consumption, traction, and drivetrain behaviour, making it difficult to generalize performance metrics across different operations [2,5]. Accurate modelling must therefore incorporate task-specific parameters and adapt to changing workloads to ensure realistic simulation outcomes [1].

Experimental validation of vehicle longitudinal dynamics provides a fundamental basis for further vehicle development, system upgrades, and simulation-based analyses [20]. By combining multi-body modelling with measured vehicle motion data, such validation ensures that the model reliably represents real-world behaviour, independent of specific drivetrain configurations [21]. A systematic framework for vehicle dynamics model validation is often employed, emphasizing the definition of validation metrics, iterative comparison between simulated and measured responses, and careful estimation of vehicle parameters during dynamic tests [22]. This approach supports the extension of the validated framework to evaluate alternative drivetrains, hybridization strategies, and energy-efficient design modifications.

As the agricultural sector continues to adopt hybrid technologies, further advancements in vehicle modelling and data acquisition will be crucial to ensure system reliability and efficiency. Ongoing interdisciplinary collaboration—across academia, industry, and engineering domains—will be essential to refine methodologies and address the unique challenges posed by off-road conditions [14,23]. With rising demand for energy-efficient, environmentally friendly agricultural machinery, the next generation of hybrid vehicles will rely heavily on validated models capable of simulating real-world conditions with precision and reliability [7,15].

To address the need for accurate and validated vehicle models in applied engineering contexts, this study presents an experimental investigation of the Claas Xerion 3800 tractor as a reference platform for vehicle-level longitudinal model validation, using a continuously variable transmission (CVT) drivetrain. The experiment was designed to determine key vehicle response parameters—rolling resistance coefficient, engine loads and drivetrain-related boundary properties—and to assess the accuracy of a simulation model by comparing it with measured operational real-world data. Through coast-down testing, diagnostic data acquisition, and fuel consumption analysis, the study aims to establish a drivetrain-independent modelling and validation framework intended to serve as a reliable baseline that can support future applications such as subsequent drivetrain optimization studies, including future hybrid system integration and energy-efficient vehicle design.

2. Materials and Methods

This section presents the experimental setup and data acquisition procedures used to support physical modelling of the vehicle. Experiments were conducted using a Claas Xerion 3800 tractor (Harsewinkel, Germany) under controlled operating conditions, including stationary, coasting, and steady-state modes. The study aimed to collect vehicle motion, drivetrain, and environmental data, as well as parameters such as vehicle mass, tire–ground contact area, transmission ratios, and rolling resistance. Data were obtained using GPS-based logging, onboard diagnostics, external measuring instruments, and software processing tools, providing the inputs required for model validation and assessment of longitudinal vehicle behavior.

2.1. Vehicle Description and Experimental Setup

To validate the physical model of the vehicle, an experiment is conducted in which operational parameters and data are collected. These data enable the determination of the actual resistance forces acting on the vehicle, as well as the identification of physical parameters related to the vehicle itself and its interaction with the environment. Limiting geometric and operational variability during validation enables isolation of longitudinal response characteristics, facilitating consistent baseline comparison and subsequent extension to alternative drivetrain configurations. The experiment utilizes the Claas Xerion

3800 (see Figure 1, Table 1) tractor—the same tractor that serves as the basis for the hybrid drivetrain modelling [24].

Figure 1. The Claas Xerion 3800 used for the experimental test drives.

Table 1. Main specifications of the Claas Xerion 3800.

Vehicle Mass	13,019.3 kg	
Engine Cat 9 ACERT	Fuel Type	Diesel
	Displacement	8.82 L
	Max. Power	254 kW
Transmission ZF ECCOM 3.5	CVT	
	Max. Speed	50 km/h
Wheels	900/60 R38	
	Tire Pressure	1.5 bars
	Contact Area	0.7982 m^2

Accordingly, the experimental data were used to generate a CVT map, which serves as an input for the vehicle-level longitudinal model, and the main components of the vehicle remain unchanged (see Table 1).

The components of the tractor utilized in both operation and simulation are thoroughly detailed in the parameter Table 1. The physical model was implemented in AVL CRUISE (v2020.1) using a conventional four-wheel-drive CVT vehicle model. Input vehicle data not included in Table 1 and not obtained during the described experimental runs were taken from manufacturer specifications. Default implicit Euler solver settings were used, and no user-built or custom modules were included.

During the experiment, the ambient temperature was 12 °C, and the wind speed was 5.6 m/s west. The wind direction was perpendicular to the track and acted symmetrically across both driving directions; therefore, its net effect was considered negligible. The vehicle's operating modes are presented in Table 2.

During stationary operating modes, external measurements are performed. Vehicle mass (see Table 1) is determined using stationary vehicle scales. Off-road vehicle tire traction characteristics differ from those of road tires, making standard contact area estimation methods less accurate. To determine the actual contact area, the vehicle was stopped on undisturbed moist sandy soil with tire pressure set to 1.5 bar. Since all wheels are the same

size and weight distribution is nearly even (47/53) [25], measurements were taken from a single wheel. The contact patch dimensions were approximately 800 mm in length and 850 mm in width. Tread imprint depth ranged from 30 mm in the centre to 50 mm at the edges. A 3D model of the tire imprint was created, yielding a calculated contact area of 0.7982 m^2—a lower than the preliminary set value of 0.9884 m^2 (Figure S1).

Table 2. Operating modes.

Mode	Speed, km/h	Data Received
Stationary	-	Vehicle mass, wheel contact area
Acceleration and coasting	30/15	Determination of the rolling resistance coefficient
Steady-state operating modes	14/12/10/7	CVT ratio map

2.2. Data Acquisition and Load Determination

While the vehicle is in acceleration and coasting modes, data are collected on its dynamic behaviour during acceleration and its inertia during deceleration. From the collected data, the rolling resistance coefficient is calculated and used for model validation. During steady-state operating modes, data are also gathered on the vehicle's dynamic performance when reaching, transitioning to, and maintaining constant operating speeds. Additionally, data are collected to determine the relationship between the internal combustion engine and the transmission ratios.

The experimental driving tests consist of two main types of runs—acceleration and coasting—as well as steady-state operating intervals (Figure 3a,b). Data collection is carried out using a data logger, diagnostic equipment, an onboard computer, and a timer. Additional parameters are determined using scales and metric measuring instruments. Data processing is performed using the software tools Race Technology (v.8.5), Matlab (v.2024a), and SolidWorks (v.2020). The sequence diagram of the equipment used during the experimental studies for determining the main operating parameters and the rolling resistance coefficient is shown in Figure 2. The experimental setup include: A—time-speed driving cycle; B—GPS signal; C—Claas Xerion 3800 tractor; D—OBD protocol connector; E—DL1 data logger; F—TEXA diagnostic software; G—laptop computer; H—Matlab software; I—CVT map; J—rolling resistance coefficient values. In Figure 2 there are shown three data sets that was collected during the tests. The dataset marked A is the speed-time data collected during the coast down run with 30 km/h maximum speed; the dataset I is the CVT map constructed from collected datapoints; J is the dataset of calculated rolling resistance values during the same coasting procedure shown in the dataset A.

To collect data such as vehicle position, speed, and acceleration, the GPS data logger Race Technology DL1 (Eastwood, England) is used. The data logger measures speed using both GPS signals and an accelerometer, resulting in a measurement accuracy of greater than 0.1%. Measurement results are recorded at a frequency of 0.01 s [26]. Since the vehicle's position is also recorded, the Race Technology software allows for precise determination of the vehicle's global position (up to 2 m), which also enables identification of the direction in which the vehicle is moving at any given moment. The data collected by the logger can be reviewed and analysed using the software or exported into file formats compatible with other data processing tools, such as Matlab.

Figure 3a illustrates the variation in speed over time recorded during the acceleration and coasting phases of the experimental drive. This data is used not only to determine rolling resistance within specific time intervals (Figure 4), but also to validate the physical model (Figures 6–8) as a complete speed–time cycle. It captures both acceleration and braking characteristics, as well as the natural motion of the tested vehicle.

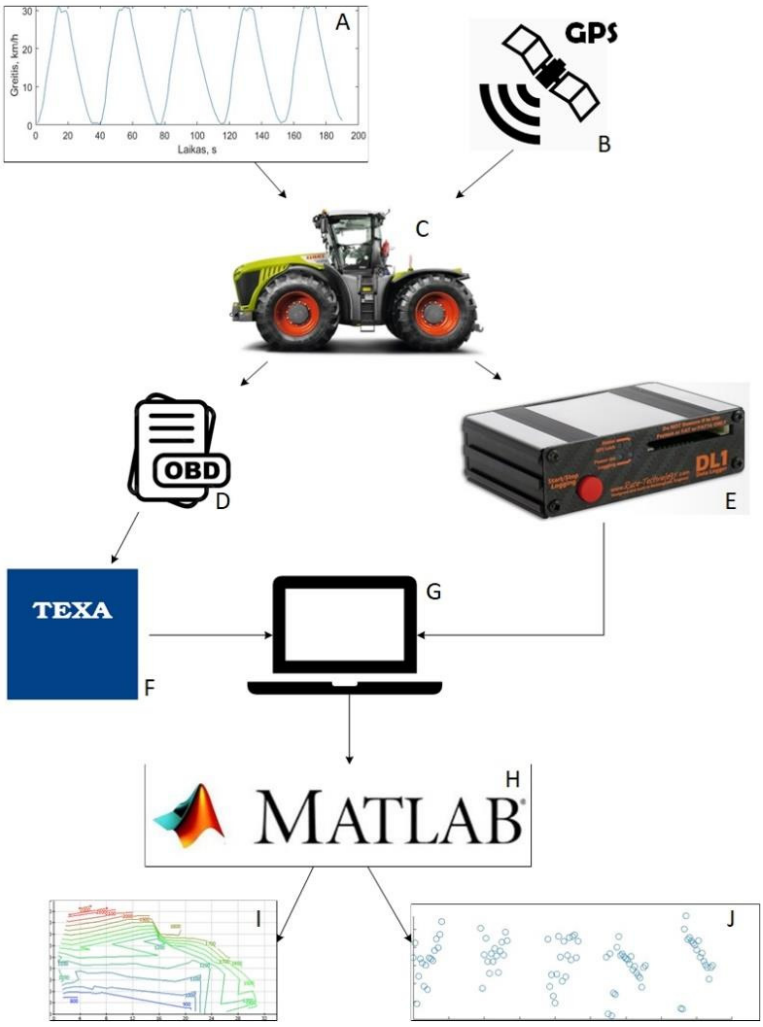

Figure 2. Experimental setup schematic diagram.

Engine operating data (Figure 3b) are retrieved using the TEXA diagnostic system. This equipment functions as an equivalent to the manufacturer's diagnostic tools—by utilizing internet-based IP protocols, the software connects directly to the manufacturer's diagnostic data, enabling full access to all specific diagnostic functions of the vehicle, regardless of its type or manufacturer [27]. The engine operating parameters of the tested vehicle, along with motion data, are collected in real time and recorded in a diagnostic log. This log is later segmented into smaller time intervals and digitized using Matlab software.

Following the retrieval of engine operating parameters during both acceleration and coasting, as well as steady-state modes, a load and fuel consumption map was generated. This map is used in the physical model of the engine description to verify and refine theoretical data. It was determined that the data from the theoretical engine model maps align with the experimentally obtained engine performance data within acceptable error margins (Figures 6–8). Since the TEXA IDC5 (v23.22.a) diagnostic software does not allow access to real-time CVT operating data, the CVT map is constructed using information from the onboard computer. During both driving modes, the onboard computer's transmission ratio readings and vehicle speed are recorded. These point-wise data were synchronized using their time stamps and cross-referenced with measurements from the data logger and TEXA diagnostic equipment, allowing CVT ratio values to be assigned to each dynamic driving phase. The resulting dataset was then uploaded into AVL, which generated a CVT map for use in the physical model (Figure 2I).

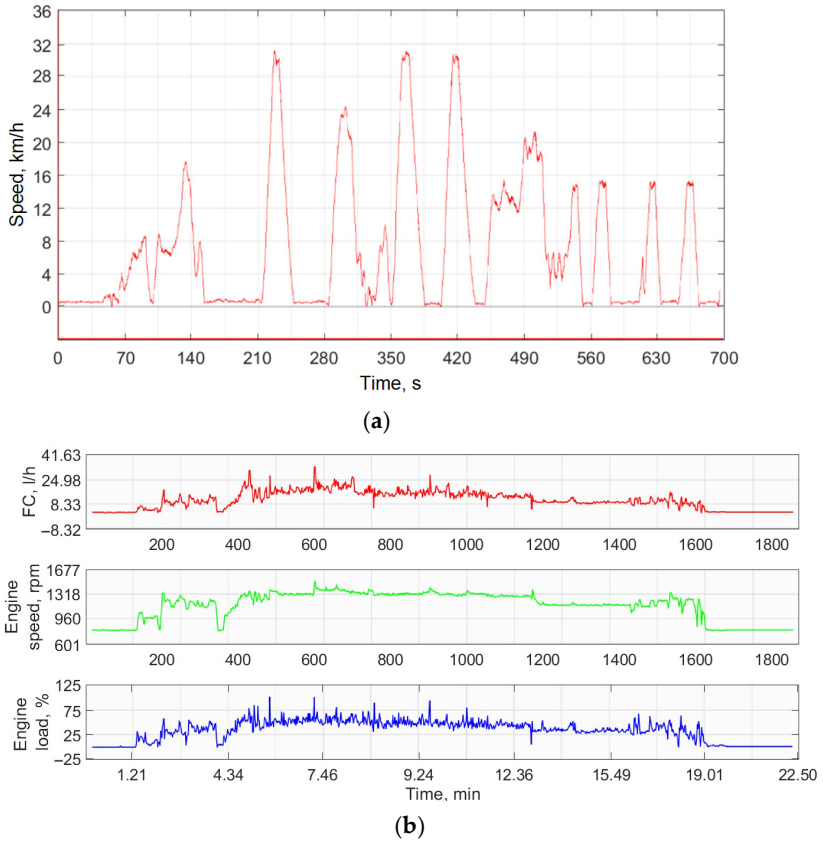

Figure 3. The experimental driving test runs: (**a**) data logger-recorded drive for the determination of rolling characteristics; (**b**) engine operating parameters in steady-state mode. TEXA report.

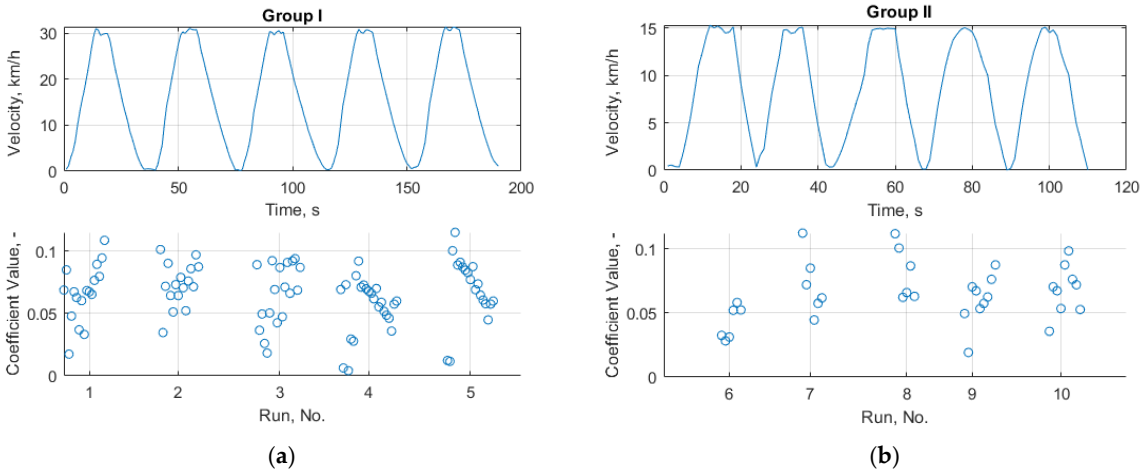

Figure 4. Instantaneous values of rolling resistance determined during the rolling experiment: (**a**) coasting after reaching 30 km/h; (**b**) coasting after reaching 15 km/h.

2.3. Determination of the Rolling Resistance Coefficient

To verify the range of values for the rolling resistance coefficient for physical modelling, a coast-down test is performed. The essence of this test is to determine the resistance forces by utilizing the inertia of the vehicle [28]. The vehicle is accelerated to a predetermined constant speed. Once the speed stabilizes, the transmission is shifted to neutral, and the vehicle coasts until it comes to a complete stop. An accelerometer records the vehicle's motion parameters. While coasting (decelerating) in neutral, the inertial force of the vehicle is equal to the sum of all resistance forces [29]. Since the influence of incline forces in this case is negligibly small, the total resistance force consists of rolling resistance and

aerodynamic drag. Knowing the vehicle speed, wind speed, and direction during the experiment, it is possible to determine the rolling resistance component of the total resistance force. Furthermore, by knowing the vehicle's mass, the rolling resistance coefficient can be calculated by the following equations [30]:

$$F_{t,c} = F_{res,\,c} \tag{1}$$

$$F_{t,c} = m_v \cdot a_d \tag{2}$$

$$F_{res,\,c} = F_a + F_{rr,c} \tag{3}$$

$$F_{rr,c} = c_w\left(1 + \frac{v_v}{100}\right)\cdot G_v \tag{4}$$

where $F_{t,c}$—traction force; $F_{res,\,c}$—total resistance; m_v—experimentally obtained vehicle mass; a_d—coasting deceleration; F_a—aerodynamic drag; $F_{rr,c}$—rolling resistance force; c_w—rolling resistance coefficient; v_v—coasting velocity; G_v—vehicle weight.

This experiment aims to determine the average value of the rolling resistance coefficient c_w, which is used for validating the physical model based on experimental data. To determine the average rolling resistance coefficient c_w, a coast-down test was conducted using the Claas Xerion 3800 tractor. Data were collected using a GPS data logger and accelerometer, with supplementary measurements from diagnostic software and onboard instrumentation. The collected data were processed using Matlab and Race Technology software to extract instantaneous acceleration and speed values, which were then used to calculate the rolling resistance coefficient. Ten coast-down runs were performed—at a constant speed of 30 km/h (Group I) and at 15 km/h (Group II) (Figure 4). Since the physical model incorporates load, speed, and pressure coefficients, which respectively influence the value of the main coefficient c_w, the experiment seeks to determine an average value that is suitable for both low and higher vehicle speeds (see Figure 4a,b). The runs were conducted in different directions to eliminate the potential influence of additional wind resistance. Repeating the experiment not only allows for a more accurate determination of the average coefficient value but also reveals the range of the c_w coefficient when the road surface exhibits variable characteristics that influence rolling resistance, including composition, moisture content, compaction, and other surface properties affecting tyre–ground interaction [31]. In this study, statistical robustness is achieved through repeated coast-down runs combined with median-based aggregation and distributional analysis of the derived c_w values, which reduces sensitivity to outliers and captures run-to-run variability without assuming normality.

3. Results of Rolling Resistance Coefficient Analysis and Vehicle Model Validation

This section presents the results obtained from the experimental study and subsequent model validation of the agricultural vehicle system. The rolling resistance coefficients determined from repeated coast-down tests are analyzed to characterize the vehicle resistance behavior under different operating speeds. Data from the experiments are then used to validate the physical vehicle model, including acceleration, traction forces, and fuel consumption, by comparing simulated outputs with measured values. Statistical and visual analyses are applied to assess the consistency, variability, and reliability of the results across different runs and operating conditions.

3.1. Rolling Resistance Coefficient Analysis

The distribution of the rolling resistance coefficients calculated from the coast-down tests are presented in Figure 4, which shows the instantaneous values of rolling resistance

during the deceleration phase for both speed groups. To determine the coefficient, five coast-down runs were performed at a constant speed of 30 km/h (Group I, Figure 4), and five runs at a constant speed of 15 km/h (Group II, Figure 4).

Since Group I tests are conducted at a higher constant vehicle speed, each run yields a larger sample of values compared to Group II. Additionally, due to the lower maximum speed in Group II, not only is the sample size reduced, but greater fluctuations in the acceleration vector are observed, which in some cases further reduces the sample size. In Group I, the values are distributed relatively evenly, with minor deviations at the beginning or end of the value range. In Group II, greater variability is observed in individual cases; however, the clustering of values generally follows similar trends as in Group I. Certain deviations in value clusters are observed in both groups—specifically, Run 3 in Group I and Run 1 in Group II. To more accurately assess the reliability of the data, a statistical analysis is performed, determining the median, quartiles, and confidence coefficient for each run. The results of the data analysis are presented in Figure 5.

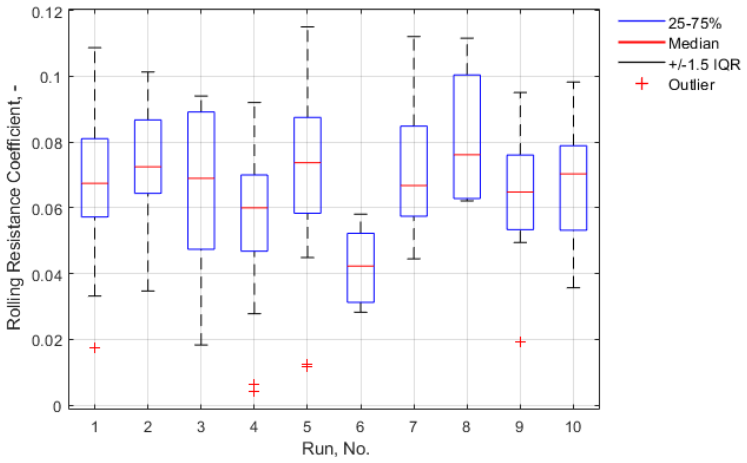

Figure 5. Rolling resistance coefficient values determined through the rolling experiment.

Figure 5 includes Group I runs (Runs 1–5) and Group II runs (Runs 6–10). The red line represents the median of the rolling resistance coefficient values calculated during each run. The blue rectangle indicates the interquartile range (25th–75th percentiles) of the coefficient values. The full data range, excluding values that do not follow the distribution trend, is marked by the ends of the dashed lines. Red "+" symbols indicate extreme values, which reflect data deviations and correspond to points removed by applying a 5–95 percentile filter.

Among all the test runs, Run 6 stands out statistically, with a median value of 0.042, while the medians of all other runs fall within the range of [0.060–0.076]. A wider cluster of value in Run 3 are visible in Figure 5. A similar distribution is observed in Run 8; however, in both cases, the median values of the calculated coefficients are close to those of the other runs, and thus these runs are included in the overall coefficient determination. In contrast, the median value of Run 6 lies more than 1.5 times the interquartile range below the 25th percentile of all runs, satisfying a standard statistical criterion for identifying outliers. Since the results of Run 6 deviate from the general range of median values both in terms of average and overall spread, this run is excluded from the calculation of the average rolling resistance coefficient c_w. The deviations observed in Runs 1, 4, 5, and 9 remain below the 0.02 threshold. As seen in Figure 4, these values occur at the beginning of the coast down phase, suggesting that they are influenced by residual effects from the vehicle's propulsion system—since even when maintaining a constant speed, minimal acceleration changes are still present. A similar cause explains the relatively high coefficient values

c_w > 0.10 observed in Runs 1, 5, 7, and 8, which occur when the direction of the vehicle's acceleration vector has just changed and has not yet stabilized. These values are regarded as a natural consequence of the initial coast-down phase and are therefore retained in the overall coefficient calculation but are weighted by a factor of 0.5 to reduce their influence relative to values within the 25th–75th percentile range.

Based on the analysis of all runs except Run 6, the overall rolling resistance coefficient is calculated to be 0.069. If Run 6 were included, the average value would be 0.0682, indicating that even with one of the larger data deviations, the overall value remains close to the 0.070 threshold. This consistency in the average value is also reflected in the percentile distribution shown in Figure 5. The spread of the distribution reflects experimental variability across ten repeated coast-down runs.

3.2. Validation of the Vehicle Model

Based on experimentally determined data, the vehicle model is validated. A CVT (Continuously Variable Transmission) drive map is created, based on a gear ratio map established during testing. General vehicle characteristics and resistance forces identified during testing are also used. The simulation is performed by transferring the vehicle movement recorded with a GPS data logger during the experiment into the simulation environment as a computed driving cycle (Figure 2E). During the simulation, like in the experiment, the forces acting on the vehicle, the accelerations affecting the vehicle, and the engine operating parameters are determined. The model validation is defined successful if validation parameters deviate less than 5% between simulated and measured data [21,32].

The parameters calculated during the simulation, reflecting the overall movement of the vehicle, essentially coincide with the experimentally derived motion criteria—the vehicle's longitudinal acceleration a_v nearly matches exactly, with only minor differences observed in the experimental peaks (Figure 6a). A similar result is obtained when comparing the instantaneous traction force $F_{t,i}$—visually, a slightly greater fluctuation in the amplitude of the experimental data is observed (Figure 6b); however, overall, the results are consistent (Figure 7).

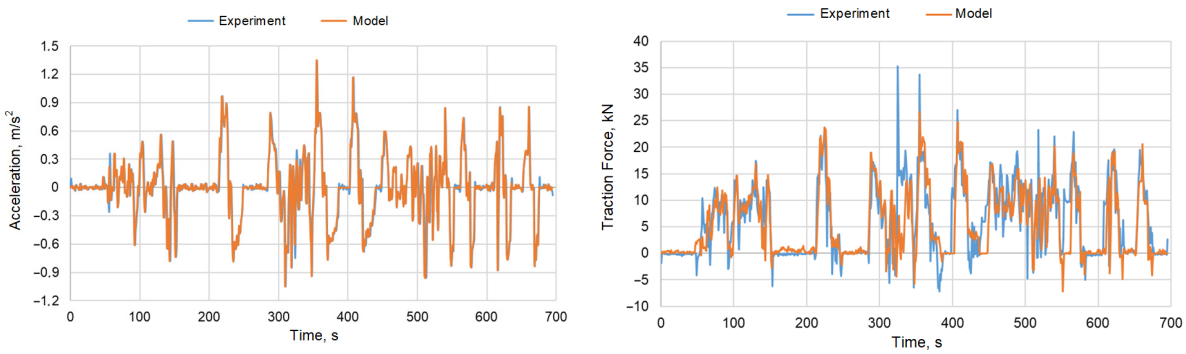

Figure 6. Comparison of Experimental and Simulation Results of Vehicle Movement: (**a**) Vehicle acceleration during the test; (**b**) Traction force attainable by the vehicle.

In both cases, the peaks observed in the experimental data on the graphs may be the result of variable resistance forces during movement. The results of the vehicle's longitudinal acceleration from the experimental and physical models do not show any other visual discrepancies. In Figure 6b, the traction force also shows a different distribution of force vectors during the experimental drive in the 320–338 s time interval. Therefore, to ensure the reliability of the results, additional statistical data comparison is performed. For this, Matlab was used to compute cumulative probability curves directly from the

experimental and model traction force samples. Both data sets are presented as cumulative probability curves along with the confidence interval boundaries for each set (Figure 7). Since the overall match of the results falls within the 5–95% confidence interval limits, it is assumed that the coincidence between the experimental and physical modelling results is sufficient.

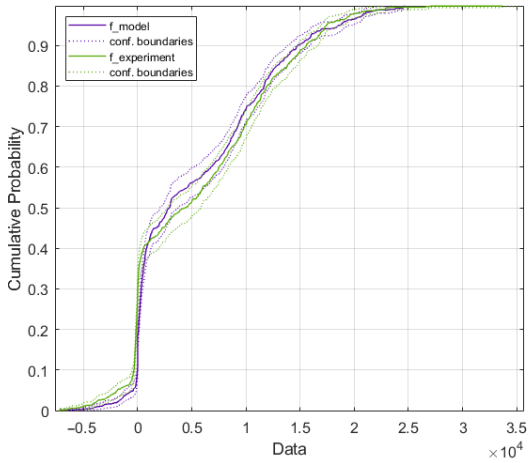

Figure 7. Cumulative probability of the traction force samples.

Although the same CVT map, recorded during the experimental drive, is used for modelling, the internal combustion engine operates under slightly different controls during the experiment and the simulation. This operational difference is reflected in the comparison of instantaneous fuel consumption (Figure 8). Nevertheless, the total amount of fuel consumed in both cases differs only slightly—by 2.1% from 2.51 kg during simulation to 2.56 kg during the experimental run. The per-step mean absolute error is 0.018 kg, further confirming agreement at each timestep. In the simulation, the instantaneous fuel consumption reaches significantly higher peak values, as the engine load fluctuates from idle to maximum load. In contrast, during the experiment, despite variations in momentary load, the engine operates within a relatively narrow load range and does not approach idle conditions. However, the fuel consumption profile generated by the simulation closely aligns with the experimental data, as shown in Figure 8. Despite the step-like nature of the model output, the cumulative fuel consumption over time remains consistent with the experimentally observed values, which exhibit a smoother result. This visual and quantitative agreement substantiates the previously established similarity in fuel consumption behaviour.

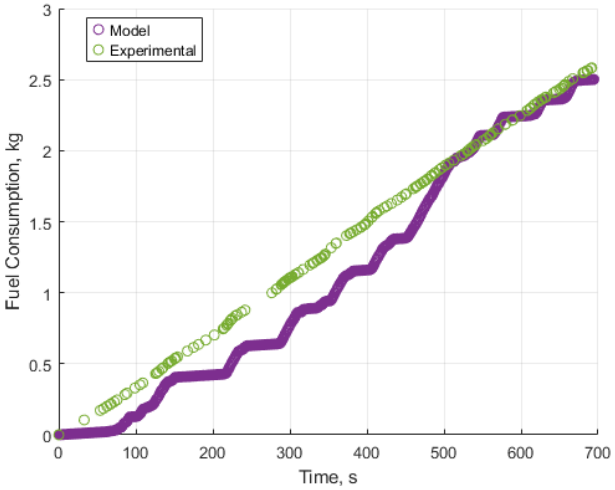

Figure 8. Comparison of Theoretical and Experimental Fuel Consumption.

4. Discussion

This study aimed to validate a physical model of a continuously variable transmission (CVT) drivetrain under realistic operating conditions, with the broader goal of improving simulation accuracy for vehicle performance and energy efficiency applications. The motivation stems from the need for reliable models in agricultural contexts, were off-road dynamics and variable loads challenge conventional drivetrain simulations.

The validation process confirmed that the model accurately replicates key vehicle behaviours, including longitudinal acceleration, traction force, and fuel consumption. The rolling resistance coefficient, determined using repeated coast-down runs and a median-based aggregation approach, provided a dependable input for simulation. The close alignment between experimental and simulated fuel consumption—differing by only 2.1%—further supports the model's predictive capability.

These results demonstrate the model's suitability for use in drivetrain optimization, hybrid system integration, and energy-efficient design. By grounding the simulation in experimentally verified data, the study contributes a reliable framework for future research and practical applications in vehicle engineering.

5. Conclusions

This study successfully validated a physical model of a CVT-equipped agricultural vehicle through a structured experimental and simulation-based approach. The key outcomes are as follows:

- A statistically robust rolling resistance coefficient of c_w = 0.069 was determined using repeated coast-down tests and a median-based aggregation method, minimizing the influence of outliers and capturing run-to-run variability across test conditions.
- Simulated vehicle dynamics—including longitudinal acceleration and traction force—closely matched experimental data, confirming the model's accuracy in replicating real-world behaviour.
- Fuel consumption analysis revealed a strong agreement between simulation and experiment, with only a 2.1% deviation in total fuel usage, despite differences in instantaneous load profiles.
- The integration of GPS data logging, diagnostic software, and CVT mapping enabled high-accuracy modelling of vehicle behaviour under realistic operating conditions.

These findings demonstrate the effectiveness of the proposed validation methodology and support its application as a validated baseline for drivetrain optimization studies, including future hybrid system integration and energy-efficient vehicle design.

Supplementary Materials: The following supporting information can be downloaded at: https://www.mdpi.com/article/10.3390/app16041814/s1, Figure S1: 3D model of the tire-ground contact area.

Author Contributions: Conceptualization U.K.M., R.M. and V.L.; Methodology, U.K.M. and R.M.; Software, U.K.M. and A.L.; Validation, U.K.M.; Formal Analysis, U.K.M.; Investigation, U.K.M.; Resources, R.M. and V.L.; Data Curation, U.K.M.; Writing—Original Draft Preparation, U.K.M.; Writing—Review & Editing, U.K.M. and R.M.; Visualization, U.K.M.; Supervision, R.M. and V.L.; Project Administration, R.M.; Funding Acquisition, R.M. and V.L. All authors have read and agreed to the published version of the manuscript.

Funding: This research received no external funding.

Data Availability Statement: The raw data supporting the conclusions of this article will be made available by the authors on request.

Acknowledgments: The authors thank AVL company for the opportunity to use the vehicle system and driveline simulation tool AVL CRUISE, which was used to simulate the hybrid and CVT drive-

train behaviour in the same conditions as the experiment was performed. A cooperation agreement has been concluded between the faculty of the Transport Engineering of Vilnius Gediminas Technical University and AVL Advanced Simulation Technologies.

Conflicts of Interest: The authors declare no conflict of interest.

References

1. Tebaldi, D.; Zanasi, R. Modeling Control and Simulation of a Parallel Hybrid Agricultural Tractor. In Proceedings of the 2021 29th Mediterranean Conference on Control and Automation (MED), Puglia, Italy, 22–25 June 2021; pp. 317–323. [CrossRef]
2. Yang, Y.; Wen, Y.; Sun, X.; Wang, R.; Dong, Z. A Review of Green Agriculture and Energy Management Strategies for Hybrid Tractors. *Energies* **2025**, *18*, 3224. [CrossRef]
3. Thornton, M.; Ratcliff, M.; Kelly, K. *Off-Road Vehicle Decarbonization and Energy Systems Integration: R&D Gaps and Opportunities*; National Renewable Energy Laboratory (NREL): Golden, CO, USA, 2022.
4. Zhu, Z.; Hou, R.; Zhang, H.; Wang, D.; Chen, L. Multi-objective optimization of design parameters for tractor hydro-mechanical continuously variable transmissions. *Sci. Rep.* **2025**, *15*, 13261. [CrossRef] [PubMed]
5. Un-Noor, F.; Wu, G.; Perugu, H.; Collier, S.; Yoon, S.; Barth, M.; Boriboonsomsin, K. Off-road construction and agricultural equipment electrification: Review, challenges, and opportunities. *Vehicles* **2022**, *4*, 780–807. [CrossRef]
6. Yue, H.; Lin, J.; Dong, P.; Chen, Z.; Xu, X. Configurations and control strategies of hybrid powertrain systems. *Energies* **2023**, *16*, 725. [CrossRef]
7. Guzzella, L.; Sciarretta, A. *Vehicle Propulsion Systems: Introduction to Modeling and Optimization*; Springer: Berlin/Heidelberg, Germany, 2005.
8. Martini, V.; Mocera, F.; Somà, A. Design and experimental validation of a scaled test bench for the emulation of a hybrid fuel cell powertrain for agricultural tractors. *Appl. Sci.* **2023**, *13*, 8582. [CrossRef]
9. McDavid, R.; Koci, C.; Bazyn, T.; Steffen, J.; Kruiswyk, R.; Duvall, L.; Adams, J.; Waldron, T. *Hybrid Heavy Duty Diesel Powertrain for Off-Road Applications (Final Technical/Scientific Report)*; Caterpillar Inc.: Deerfield, IL, USA, 2023.
10. Smithm, D.; Ozpineci, B.; Graves, R.L.; Jones, P.T.; Lustbader, J.; Kelly, K.; Walkowicz, K.; Birky, A.; Payne, G.; Sigler, C.; et al. *Medium-and Heavy-Duty Vehicle Electrification: An Assessment of Technology and Knowledge Gaps*; Oak Ridge National Laboratory (ORNL): Oak Ridge, TN, USA, 2020.
11. Koci, C.; Steffen, J.; Kruiswyk, R.; Guo, F.; Bazyn, T.; McDavid, R.; Ivanov, R.; Sirimalla, D. *A Hybrid Heavy-Duty Diesel Power System for Off-Road Applications-Concept Definition*; SAE Technical Paper, 0148–7191; SAE International: Warrendale, PA, USA, 2021.
12. El-Gindy, M.; El-Sayegh, Z. *Road and Off-Road Vehicle Dynamics*; Springer: Cham, Switzerland, 2023.
13. Reina, G.; Milella, A.; Galati, R. Terrain assessment for precision agriculture using vehicle dynamic modelling. *Biosyst. Eng.* **2017**, *162*, 124–139. [CrossRef]
14. Mi, C.; Masrur, M.A. *Hybrid Electric Vehicles: Principles and Applications with Practical Perspectives*; John Wiley & Sons: Hoboken, NJ, USA, 2025.
15. Husain, I. *Electric and Hybrid Vehicles: Design Fundamentals*; CRC Press: Boca Raton, FL, USA, 2021.
16. Musau, H.; Ruganuza, D.; Indah, D.; Mukwaya, A.; Gyimah, N.K.; Patil, A.; Bhosale, M.; Gupta, P.; Mwakalonge, J.; Jia, Y.; et al. A Review of Off-Road Datasets, Sensor Technologies and Terrain Traversability Analysis. *SAE Int. J. Adv. Curr. Pract. Mobil.* **2025**, *7*, 2568–2588. [CrossRef]
17. Pascuzzi, S.; Łyp-Wrońska, K.; Gdowska, K.; Paciolla, F. Sustainability evaluation of hybrid agriculture-tractor powertrains. *Sustainability* **2024**, *16*, 1184. [CrossRef]
18. Europea, U.-U. Long-term low greenhouse gas emission development strategy of the European Union and its Member States. In Proceedings of the United Nations Framework Convention on Climate Change, Online, 23 November–4 December 2020.
19. Golanbari, B.; Mardani, A.; Farhadi, N.; Reina, G. Machine learning applications in off-road vehicles interaction with terrain: An overview. *J. Terramech.* **2024**, *116*, 101003. [CrossRef]
20. Agarwal, A.; Mthembu, L. FE Structural Analysis and Experimental Investigation of HMV Chassis. In *Emerging Trends in Mechanical and Industrial Engineering; Lecture Notes in Mechanical Engineering*; Springer: Singapore, 2023; pp. 931–943. [CrossRef]
21. Ahmad, F.; Mazlan, S.A.; Zamzuri, H.; Jamaluddin, H.; Hudha, K.; Short, M. Modelling and validation of the vehicle longitudinal model. *Int. J. Automot. Mech. Eng.* **2014**, *10*, 2042–2056. [CrossRef]
22. Widner, A.; Tihanyi, V.; Tettamanti, T. Framework for Vehicle Dynamics Model Validation. *IEEE Access* **2022**, *10*, 35422–35436. [CrossRef]
23. Kumar, A.; Kumar, P.; Letha, S.S. *Smart Electric and Hybrid Vehicles: Advancements in Materials, Design, Technologies, and Modeling*; John Wiley & Sons: Hoboken, NJ, USA, 2024.
24. Medževeprytė, U.K.; Makaras, R.; Lukoševičius, V.; Kilikevičius, S. Application and Efficiency of a Series-Hybrid Drive for Agricultural Use Based on a Modified Version of the World Harmonized Transient Cycle. *Energies* **2023**, *16*, 5379. [CrossRef]

25. CLAAS KGaA mbH Repair Manual. Xerion 3800-3300. Available online: https://www.claas.com/zh-cn (accessed on 7 February 2026).
26. Race Technology DL1 Data Logger Datasheet. Available online: https://www.race-technology.com/upload/DL1_Dsheet.pdf (accessed on 8 August 2025).
27. TEXA. TEXA S.p.A.—Navigator TXT MULTIHUB. Available online: https://www.texa.com/products/navigator-txt-multihub/ (accessed on 19 February 2024).
28. Suyabodha, A. A relationship between tyre pressure and rolling resistance force under different vehicle speed. *MATEC Web Conf.* **2017**, *108*, 12004. [CrossRef]
29. SAE. *ETA-HTP01 Revision 2 Effective February 1, 2008 Implementation of SAE Standard J2263 "Road Load Measurement Using Onboard Anemometry and Coastdown Techniques"*; SAE International: Warrendale, PA, USA, 2008. Available online: https://www.energy.gov/sites/prod/files/2015/04/f21/htp001r2.pdf (accessed on 15 February 2023).
30. Wiegand, B. *Estimation of the Rolling Resistance of Tires*; SAE International: Warrendale, PA, USA, 2016. [CrossRef]
31. Wong, J.Y. *Terramechanics and Off-Road Vehicle Engineering: Terrain Behaviour, Off-Road Vehicle Performance and Design*; Butterworth-Heinemann: Oxford, UK, 2009.
32. Kutluay, E.; Winner, H. Validation of vehicle dynamics simulation models—A review. *Veh. Syst. Dyn.* **2014**, *52*, 186–200. [CrossRef]